

*Rapid Commun. Mass Spectrom.* 2017, 31, 253–263  
(wileyonlinelibrary.com) DOI: 10.1002/rcm.7791

# Correlation of lipidomic composition of cell lines and tissues of breast cancer patients using hydrophilic interaction liquid chromatography/electrospray ionization mass spectrometry and multivariate data analysis

Eva Cífková<sup>1</sup>, Miroslav Lísa<sup>1</sup>, Roman Hrstka<sup>2</sup>, David Vrána<sup>3</sup>, Jiří Gatěk<sup>4</sup>, Bohuslav Melichar<sup>3</sup> and Michal Holčapek<sup>1\*</sup>

<sup>1</sup>University of Pardubice, Faculty of Chemical Technology, Department of Analytical Chemistry, Studentská 573, 53210 Pardubice, Czech Republic

<sup>2</sup>Masaryk Memorial Cancer Institute, Regional Centre for Applied Molecular Oncology, Žlutý kopec 7, 65653 Brno, Czech Republic

<sup>3</sup>Palacký University, Medical School and Teaching Hospital, Department of Oncology, I.P.Pavlova 6, 77520 Olomouc, Czech Republic

<sup>4</sup>Tomáš Baťa University in Zlín, Atlas Hospital, Department of Surgery, nám T. G. Masaryka 5555, 76001 Zlín, Czech Republic

**RATIONALE:** The goal of this work is the comparison of differences in the lipidomic compositions of human cell lines derived from normal and cancerous breast tissues, and tumor *vs.* normal tissues obtained after the surgery of breast cancer patients.

**METHODS:** Hydrophilic interaction liquid chromatography/electrospray ionization mass spectrometry (HILIC/ESI-MS) using the single internal standard approach and response factors is used for the determination of relative abundances of individual lipid species from five lipid classes in total lipid extracts of cell lines and tissues. The supplementary information on the fatty acyl composition is obtained by gas chromatography/mass spectrometry (GC/MS) of fatty acid methyl esters. Multivariate data analysis (MDA) methods, such as nonsupervised principal component analysis (PCA), hierarchical clustering analysis (HCA) and supervised orthogonal partial least-squares discriminant analysis (OPLS-DA), are used for the visualization of differences between normal and tumor samples and the correlation of similarity between cell lines and tissues either for tumor or normal samples.

**RESULTS:** MDA methods are used for differentiation of sample groups and also for identification of the most up- and downregulated lipids in tumor samples in comparison to normal samples. Observed changes are subsequently generalized and correlated with data from tumor and normal tissues of breast cancer patients. In total, 123 lipid species are identified based on their retention behavior in HILIC and observed ions in ESI mass spectra, and relative abundances are determined.

**CONCLUSIONS:** MDA methods are applied for a clear differentiation between tumor and normal samples both for cell lines and tissues. The most upregulated lipids are phospholipids (PL) with a low degree of unsaturation (e.g., 32:1 and 34:1) and also some highly polyunsaturated PL (e.g., 40:6), while the most downregulated lipids are PL containing polyunsaturated fatty acyls (e.g., 20:4), plasmalogens and ether lipids. Copyright © 2016 John Wiley & Sons, Ltd.

Breast cancer represents the most commonly diagnosed cancer and, after lung cancer, the second leading cause of cancer death in women.<sup>[1,2]</sup> The stimulation by the female hormones estrogen and progesterone plays an indispensable role in the pathogenesis of breast cancer, since the incidence in men is two orders of magnitude lower. Hormonal factors associated with age, lifestyle, or diet represent the principal cause of breast cancer, while exposure to radiation and other factors

could also be responsible in individual cases. The germ-line mutations of *BRCA1* and *BRCA2* genes involved in maintenance of genome integrity represent additional factor responsible for almost 10% of breast cancer cases. Based on the tumor phenotype assessed by immunohistochemistry and molecular profiling, breast cancer is currently divided into several types with distinct biological features and therapeutic approaches, including luminal (luminal A and luminal B), HER-2-positive and basal (triple negative) breast carcinoma. The introduction of screening with early diagnosis resulting from the use of mammograms as well as the advances in multidisciplinary management of early breast cancer encompassing surgery, adjuvant (or neoadjuvant) systemic therapy including hormonal therapy, cytotoxic chemotherapy and targeted treatment, and adjuvant radiation have resulted

\* Correspondence to: M. Holčapek, University of Pardubice, Faculty of Chemical Technology, Department of Analytical Chemistry, Studentská 573, 53210 Pardubice, Czech Republic.  
E-mail: michal.holcapek@upce.cz

in a substantial reduction in mortality.<sup>[3]</sup> However, the success of multidisciplinary management is critically dependent on early detection. Although mammography represents the principal breast cancer screening method its sensitivity depends on the size of the tumor and density of the breast tissue. The necessary exposure to radiation limits the frequency of examinations and, not infrequently, breast cancer is detected within months of prior mammography (so-called interval breast cancer). Thus, biomarkers for early detection of breast cancer that could be determined in the biological fluids, and could be performed more frequently compared to mammography, are urgently needed.

The determination of biomarkers currently represents an indispensable component of the multidisciplinary management of cancer patients.<sup>[4]</sup> Circulating biomarkers currently used, e.g., carcinoembryonic antigen (CEA) or carbohydrate antigen (CA) 15-3, are not routinely used in cancer screening and the utilization in the follow-up of patients with breast cancer is also limited. Therefore, the search for new circulating biomarkers represents an unmet medical need in breast cancer.

The relation between lipid metabolism and breast cancer development has been investigated in various studies aimed at early diagnosis, identification of biomarkers and characterization of biochemical pathways.<sup>[5–9]</sup> Increased *de novo* production of fatty acids in tumor cells is associated with proliferation, aggressiveness and other aspects of malignant transformation,<sup>[7,8,10]</sup> because polyunsaturated fatty acids (PUFA), in contrast to saturated fatty acids, are more susceptible to oxidation and may subsequently induce cell death. For this reason, the increased concentrations of saturated fatty acids, such as palmitic (16:0) and stearic (18:0) acids, has been documented in breast carcinoma.<sup>[11,12]</sup> Furthermore, arachidonic (20:4; n-6 PUFA), docosahexaenoic (22:6; n-3 PUFA) and eicosapentaenoic (20:5; n-3 PUFA) acids are highlighted in many studies, because increased abundances of n-3 PUFA have been observed in tumor tissues.<sup>[8,13–18]</sup>

Comprehensive lipidomic analysis represents a challenging task due to the different structures of individual lipid classes and different physicochemical properties, such as polarity or solubility. The coupling of liquid chromatography and mass spectrometry (LC/MS) enables the separation of individual lipids and their sensitive identification and quantification, which has been frequently used in the breast cancer lipidomic research.<sup>[10,11,19–24]</sup> Many studies have reported an increased level of lipids containing saturated fatty acyls (14:0, 16:0 and 18:0) in breast tumor tissues, which is in agreement with increased *de novo* fatty acid synthesis.<sup>[11,20,22,23]</sup> The fatty acyl profiles can be measured by GC/MS after transesterification of intact lipids, which provides basic information on the fatty acyl distribution in all lipids.<sup>[12,13,15]</sup>

At the present time, MDA is an important part of most clinical studies due to the simplification and better visualization of large datasets.<sup>[25]</sup> PCA is an unsupervised statistical method providing an important overview on the sample clustering based on similarities and differences among all molecules determined. The unsupervised HCA method using the Ward linkage criterion clusters the objects according to similarities of the distance criterion using the smallest error of sum of squares. Results are visualized using a dendrogram, which merges individual samples into

clusters starting from the smallest cluster of two up to the final cluster including all samples. The supervised OPLS-DA searches for similarities and differences between predefined two groups of samples, typically healthy compared to pathological ones.

The goal of the present work is the characterization of the lipid composition of various normal and tumor breast cell lines using HILIC/ESI-MS and GC/MS methods and identification of the most significant differences in the lipidomic compositions using MDA methods. The lipidomic composition of cell lines as the simplest model for cancer research is compared with tumor and surrounding normal tissues after breast tumor surgery to determine whether the same dysregulated lipids can be observed for both models.

## EXPERIMENTAL

### Chemicals and standards

Acetonitrile, 2-propanol, methanol (all LC/MS grade), chloroform stabilized by 0.5–1% ethanol (LC grade), ammonium acetate and sodium chloride were purchased from Sigma-Aldrich (St. Louis, MO, USA). Deionized water was prepared with a Milli-Q Reference water purification system (Millipore, Molsheim, France). *N*-Dodecanoyl-heptadecaspheing-4-enine-1-phosphatidylethanolamine (d17:1/12:0) used as an internal standard (IS) was purchased from Avanti Polar Lipids (Alabaster, AL, USA). The lipid nomenclature follows the LIPID MAPS system<sup>[26]</sup> and the shorthand notation for lipid structures.<sup>[26]</sup> Breast cell lines were maintained at the Regional Center for Applied Molecular Oncology, Masaryk Memorial Cancer Institute in the Czech Republic (see Supplementary Table S1, Supporting Information), while human breast tumor and surrounding normal tissues of ten cancer patients were obtained from the Department of Surgery, Atlas Hospital Zlín, Czech Republic.

### Sample preparation

Human cancer cell lines (Supplementary Table S1, Supporting Information) were obtained from the American Type Culture Collection (ATCC) and cultured in the recommended medium containing 10% fetal bovine serum, 0.3 mg/mL L-glutamine and 100 U/mL penicillin–streptomycin (all Invitrogen, Life Technologies, Paisley, UK) at 37°C and 5% CO<sub>2</sub>. MCF10A cells were maintained in DMEM/F12 growth media supplemented with 5% horse serum, 100 U/mL penicillin–streptomycin (all Invitrogen, Life Technologies, Paisley, UK), 20 ng/mL EGF, 0.5 mg/mL hydrocortisone, 100 ng/mL cholera toxin and 10 µg/mL insulin (all Sigma-Aldrich) at 37°C and 5% CO<sub>2</sub>.

All cell lines were grown in tissue culture plates (8–12 for each cell line, 2 biological replicates) with 100 mm diameter. During cultivation, the cells were periodically checked by microscopy and tested for Mycoplasma contamination. To form cell pellets, each plate was washed two times with ice-cold phosphate-buffered saline (PBS), then the cells were detached with cell scraper into 1 mL ice-cold PBS and subjected to centrifugation at 200 g for 10 min. Cell pellets were immediately stored at –80°C.

Cell lines were extracted using a chloroform/methanol/water system according to a modified Folch extraction.<sup>[27,28]</sup>

Briefly, 70–300 mg of cell pellets and 25  $\mu$ L of 3.3 mg/mL IS were homogenized for 3 min with 5 mL of chloroform/methanol (2:1, *v/v*) mixture and the homogenate was filtered using a coarse filter paper. Subsequently, 1 mL of 1 mol/L NaCl was added, and the mixture was centrifuged at 3000 rpm for 5 min at ambient temperature. The chloroform bottom layer (total lipid extract) containing lipids was evaporated by a gentle stream of nitrogen, redissolved in 500  $\mu$ L of chloroform/2-propanol (1:1, *v/v*) mixture and filtered using a syringe filter with regenerated cellulose with a pore size 0.45  $\mu$ m (Teknokroma, Barcelona, Spain).

Fatty acid methyl esters (FAME) were prepared from the lipid extract using sodium methoxide.<sup>[29]</sup> Briefly, 50  $\mu$ L of lipid extract and 0.8 mL of 0.25 mol/L sodium methoxide in

methanol were heated in a water bath for 10 min at 65°C. After the reaction, 0.5 mL of saturated solution of NaCl in water was added and, subsequently, FAME were extracted from the mixture using 1 mL hexane.

### LC/MS conditions

Total lipid extracts were analyzed by a LC/MS method, as described previously.<sup>[28,30]</sup> A 1290 series liquid chromatograph (Agilent Technologies, Waldbronn, Germany) was coupled with an Esquire 3000 ion trap analyzer (Bruker Daltonics, Bremen, Germany). Separation of total lipid extracts was performed on a Spherisorb Si column (250  $\times$  4.6 mm, 5  $\mu$ m; Waters, Milford, MA, USA) using a flow rate of 1 mL/min, an injection volume of 1  $\mu$ L, a column temperature of 40°C and a mobile phase gradient: 0 min – 94% A + 6% B, 60 min – 77% A + 23% B, where A was acetonitrile and B was

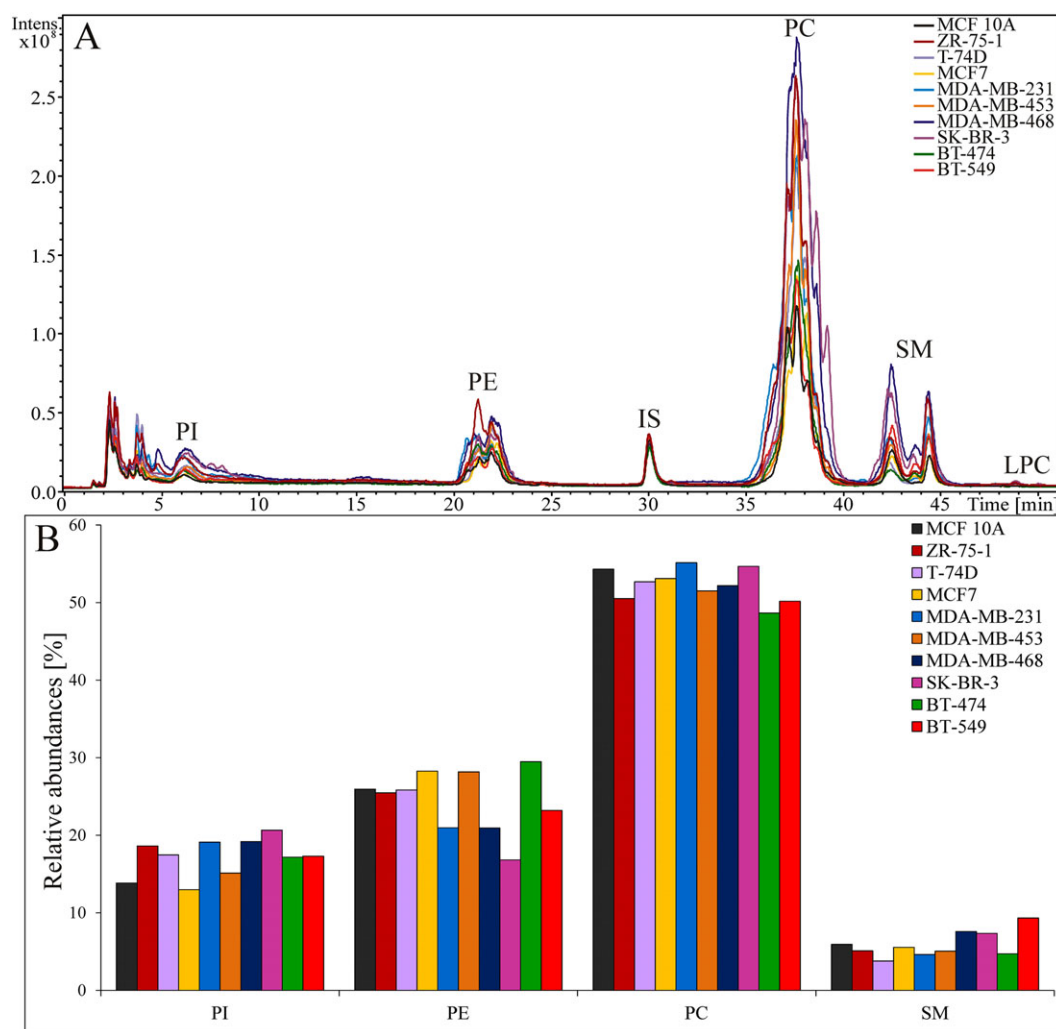


**Figure 1.** (A) Positive-ion HILIC/ESI-MS chromatograms of normal breast cell line MCF10A (black line) and nine tumor breast cell lines ZR-75-1, T-74D, MCF7, MDA-MB-231, MDA-MB-453, MDA-MB-468, SK-BR-3, BT-474, BT-549. LC conditions: column Spherisorb Si (250  $\times$  4.6 mm, 5  $\mu$ m), flow rate 1 mL/min, separation temperature 40°C, mobile phase gradient: 0 min – 94%A + 6%B, 60 min – 77%A + 23%B, where A is acetonitrile and B is 5 mM aqueous ammonium acetate. (B) Comparison of relative abundances of individual lipid classes in analyzed normal and tumor breast cell lines. Peak annotation: PI – phosphatidylinositols, PE – phosphatidylethanolamines, IS – internal standard, PC – phosphatidylcholines, SM – sphingomyelins, LPC – lysophosphatidylcholines.

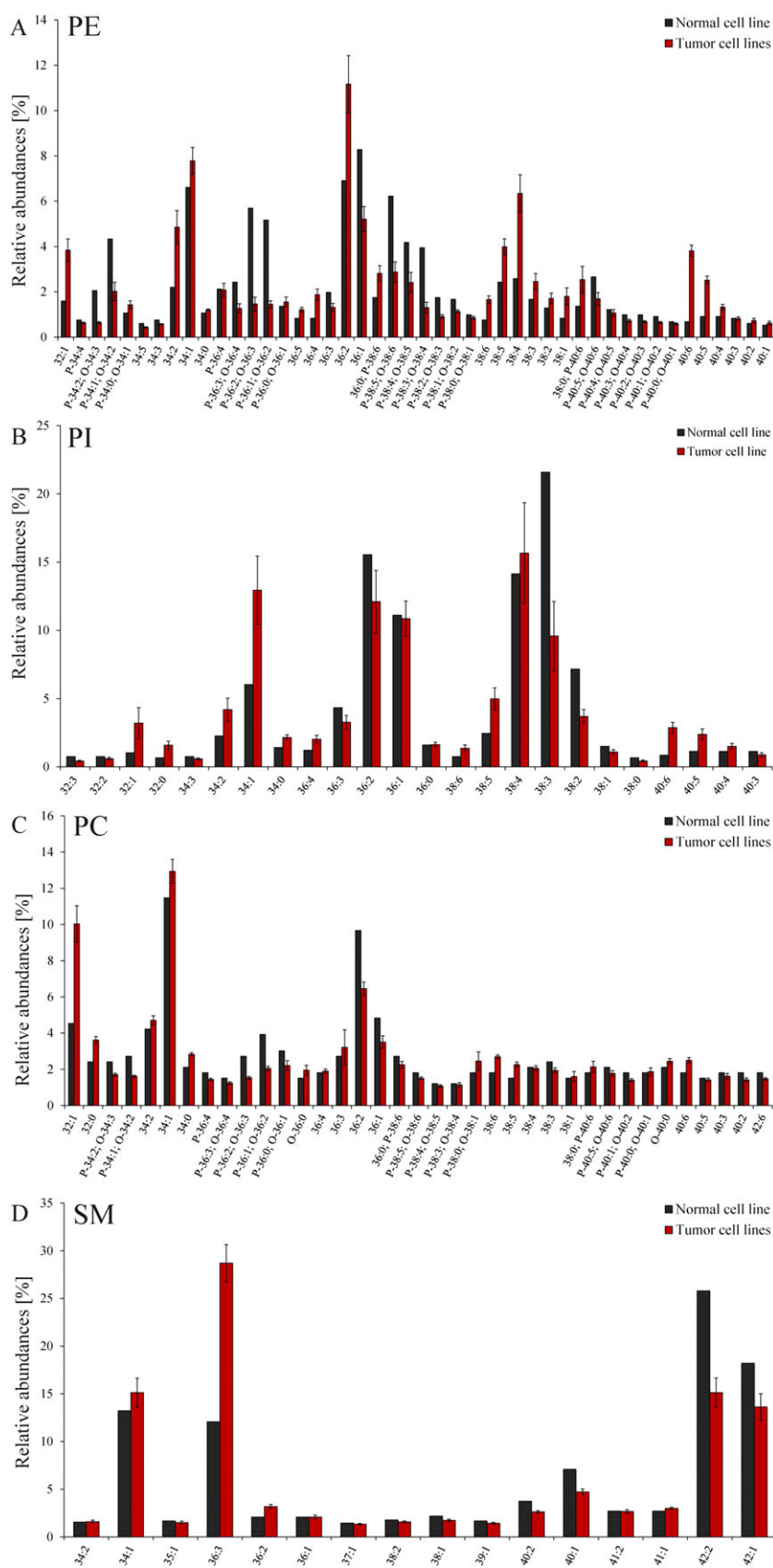


**Figure 2.** Relative abundances of individual lipids in normal breast cell line MCF10A (black columns) and average relative abundances from nine tumor breast cell lines (red columns, including standard errors of average value): (A) PE, (B) PI, (C) PC and (D) SM.

5 mmol/L aqueous ammonium acetate. Lipids were detected in positive- and negative-ion ESI-MS modes in the mass range  $m/z$  50–1000 with the nebulizing gas 60 psi, drying gas flow rate 10 L/min and drying gas temperature of 365°C. Quantitation of individual lipid classes was achieved by the single IS and response factors<sup>[30]</sup> obtained from calibration curves. Individual lipid species were identified using relative abundances of deprotonated molecules  $[M-H]^-$  for the PE and PI classes and  $[M-CH_3]^-$  ions for the PC class in the negative-ion mode. SM species were identified as protonated molecules  $[M+H]^+$  in the positive-ion mode. LPC could not be determined due to their low concentrations. Low-energy collision-induced dissociation tandem mass spectrometry (MS/MS) experiments were performed for the most abundant lipid species with an isolation width of  $m/z$  4, collision energy of 1 V and helium as the collision gas.

### GC/MS conditions

GC/MS experiments were performed on a model 7890 gas chromatograph (Agilent Technologies) using a TR-FAME column (60 m length, 0.25 mm ID, 0.25  $\mu$ m film thickness; Thermo Scientific, Waltham, MA, USA) under the following conditions: injection volume 5  $\mu$ L, split ratio 1:4 and flow rate of helium (99.996%) as a carrier gas 1.2 mL/min. The temperature gradient starting from the initial temperature 160°C, ramp to 235°C at 4°C/min and hold for 2 min, ramp to 250°C at 50°C/min. Detection was performed using a MSD 5977A quadrupole mass analyzer (Agilent Technologies) with an electron ionization (EI) source in the range  $m/z$  50–500 under the following conditions: ionization energy 70 eV, gain factor 15, isolation width  $m/z$  0.1, scanning frequency 10.9 scan/s, capillary temperature 235°C, EI source temperature 230°C and mass analyzer temperature 150°C. FAME were

identified based on retention times, mass spectra compared with the Wiley Registry of Mass Spectral Data/NIST database as well as manual interpretation.

### Statistical data analysis

MDA was performed using unsupervised HCA and PCA methods, and supervised OPLS-DA method using the SIMCA software (version 13.0; Umetrics, Umeå, Sweden). Data were preprocessed before statistical evaluation using Pareto scaling and logarithm transformation. OPLS-DA is cross-validated using leave group out method. The dendrogram was processed using the Ward linkage criterion, which minimizes the variation within the cluster. Box plots described the distribution of results using median, minimum, maximum and the variability of data sets in the first and third quartiles. Receiver operating characteristic (ROC) curves were constructed using MedCalc statistical software (version 15.8; MedCalc Software bvba, Ostend, Belgium).

## RESULTS AND DISCUSSION

### Lipidomic analysis of breast cell lines

A normal breast epithelium cell line (MCF10A) and nine breast cancer cell lines (ZR-75-1, T-74D, MCF7, MDA-MB-231, MDA-MB-453, MDA-MB-468, SK-BR-3, BT-474, BT-549, see Supplementary Table S1 (Supporting Information) for more details) were extracted according to a modified Folch procedure with chloroform/methanol/water mixture.<sup>[28]</sup> Total lipid extracts of cell lines obtained were analyzed using the HILIC/ESI-MS method. Quantitative analysis for each lipid class was performed using a combination of the single

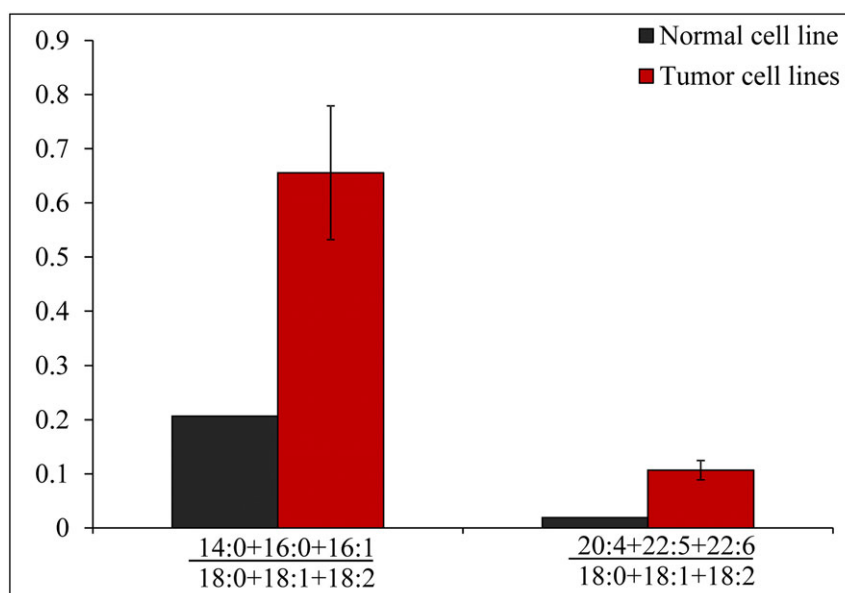


**Figure 3.** Ratios of sums of shorter acyls (14:0 + 16:0 + 16:1) to C18 acyls (18:0 + 18:1 + 18:2) and PUFA (20:4 + 22:5 + 22:6) to C18 acyls (18:0 + 18:1 + 18:2) in cell lines based on GC/MS data of FAME after the transesterification of intact lipids in normal breast cell line MCF10A (black columns) and average relative abundances from nine tumor breast cell lines (red columns, including standard errors of average value).



of double bonds. Quantitative results of PI, PE, PC and SM are reported using relative abundances in % (Fig. 1(B)), but normal and tumor cell lines do not differ substantially in their phospholipid content, therefore the detailed analysis of individual lipid species inside classes is performed using

characteristic ions in ESI mass spectra obtained by the peak integration of given lipid class in the HILIC chromatogram. The analysis of lipid species allows the characterization of relative abundances of 46 PE, 24 PI, 37 PC and 16 SM in normal and tumor cell lines (Supplementary Table S2 and Figs. S1–S4,

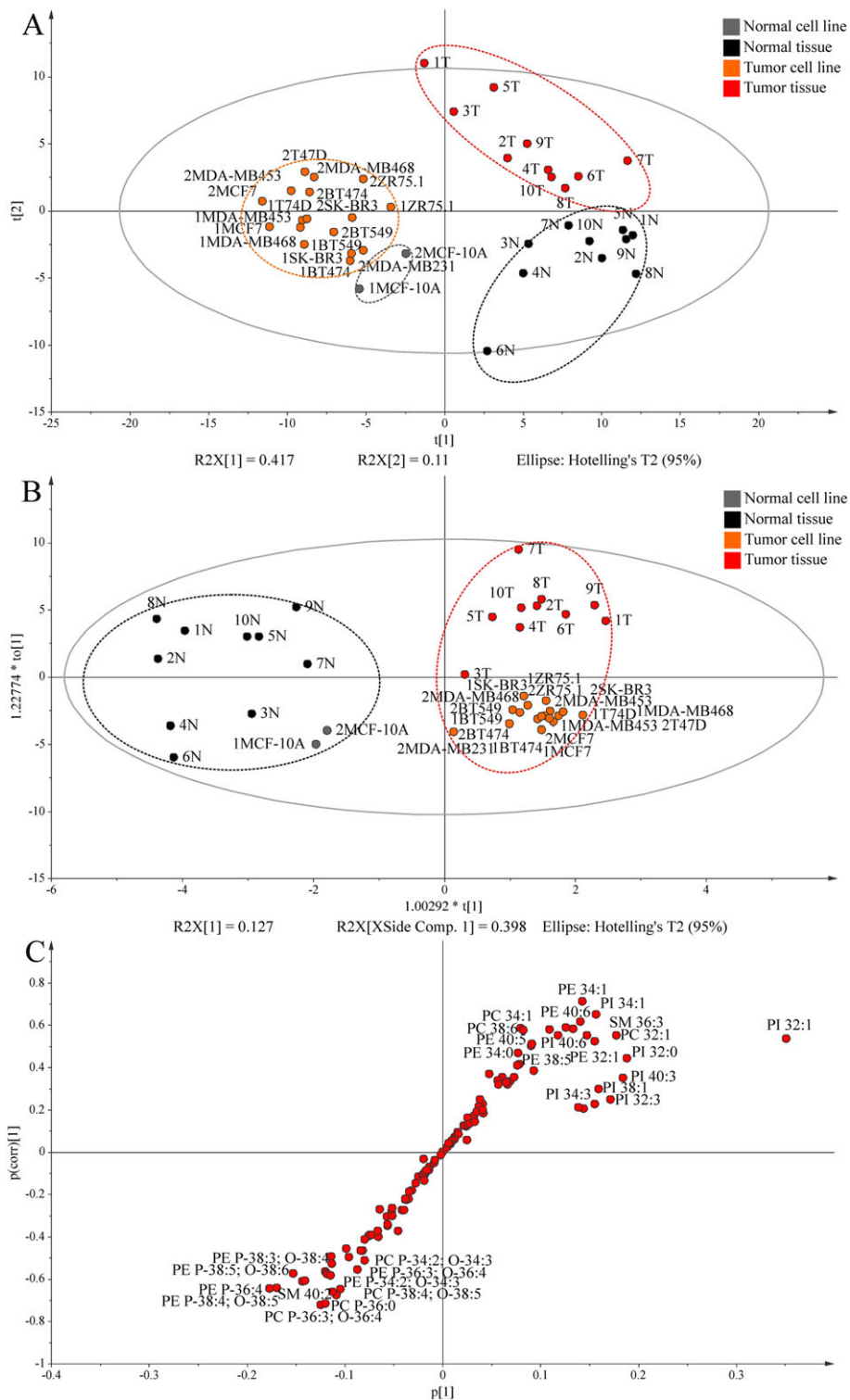


**Figure 5.** Multivariate data analysis of relative abundances of all lipids in normal and tumor breast cell lines and tissues of breast cancer patients: (A) the score plot of unsupervised PCA method, (B) the score plot, and (C) the S-plot of supervised OPLS-DA method.

Supporting Information). Figure 2 shows the comparison of relative abundances of individual lipid species inside lipid classes in the normal breast epithelial cell line and mean values for nine tumor breast cell lines. Individual lipid species are characterized by attached fatty acyls annotated by their total carbon number and double-bond number (CN:DB). Standard errors of average values are presented in figures for nine tumor samples, but they cannot be calculated for the normal sample, because only MCF10A is available. In the case of PE and PC, different types of fatty acyl linkages to the glycerol backbone in the *sn*-1 position are observed, where the ether linkage of fatty acyls in the *sn*-1 position (1-alkyl-2-acyl) is referred to as ethers (e.g., PE O-36:4) and the vinyl ether linkage in the *sn*-1 position (1-alkenyl-2-acyl) corresponds to plasmalogens (e.g., PE P-36:4). Isobaric ethers and vinyl ethers cannot be distinguished by common MS methods; therefore, we annotate them as a sum, e.g., PE P-34:2 and PE O-34:3. Figure 2 shows the significant differences between normal and tumor cell lines, which confirms the fact that tumor cells can be easily discriminated from normal cells for all studied cell lines based on their lipidomic composition. The most pronounced trend is a significant downregulation of most PE and PC ethers and plasmalogens (e.g., P-34:1/O-34:2, P-34:2/O-34:3, P-36:1/O-36:2 and P-36:2/O-36:3), while lipid species containing saturated and monounsaturated fatty acyls are significantly upregulated in tumor cell lines (e.g., species containing 34:0, 34:1, 32:1). Furthermore, lipid species containing some PUFA with more than three double bonds (e.g., 36:4, 38:4, 38:5, 38:6, 40:4, 40:5 and 40:6) are significantly upregulated in tumor cell lines. These trends are closely correlated with GC/MS results of the fatty acyl composition (Supplementary Fig. S5, Supporting Information). Saturated or monounsaturated fatty acyls with shorter acyl chains (14:0, 16:0 and 16:1) and PUFA containing four and more double bonds (20:4, 22:5, 22:6) are significantly upregulated in tumor cell lines. Plotted ratios of sums of shorter acyls to

C18 (14:0 + 16:0 + 16:1/18:0 + 18:1 + 18:2) or PUFA to C18 (20:4 + 22:5 + 22:6/18:0 + 18:1 + 18:2) show upregulation of more than 3 times for shorter acyls and more than 5 times for PUFA (Fig. 3).

### Statistical evaluation of breast cell lines data

MDA of relative abundances of detected polar lipid species was used as a tool for simplified visualization of the most significant differences between normal and tumor cell lines (Fig. 4). Cell lines were cultured, extracted and lipid composition measured using LC/MS in two batches within the time interval of 6 months (prefix 1 is the first batch, prefix 2 is the second batch, e.g., 1MCF10A and 2MCF10A) to verify the integrity of data. PCA clusters samples according to the similarities and differences between relative abundances of lipid species. Figure 4(A) shows clear clustering of the normal cell line and all tumor cell lines and significant similarities between samples in the first and second batch, providing a distinct proof of stability and reproducibility of all individual steps in sample preparation and analysis. The next step of MDA is application of the supervised OPLS-DA method (Figs. 4(B) and 4(C)), which improves the group clustering by the PCA method using predefined groups of samples (normal *vs.* tumor cell lines). The OPLS-DA score plot (Fig. 4(B)) shows excellent separation of clusters, while the S-plot (Fig. 4(C)) visualizes the lipids influencing this clustering. Upregulated lipids in tumor cell lines appear in the upper right corner and downregulated lipids in the lower left corner. The most upregulated species are PE 40:6 (PE 18:0/22:6), PE 40:5 (PE 18:0/22:5), PE 38:6 (PE 16:0/22:6), PI 40:6 (PI 18:0/22:6) and PC 32:1 (PC 16:0/16:1), and downregulated PE P-34:2 (PE P-16:0/18:2 and PE O-16:1/18:2), PE P-36:1 (PE P-18:0/18:1 and PE O-18:1/18:1), PE P-36:2 (PE P-18:0/18:2 and PE O-18:1/18:2), PC P-34:1 (PC P-18:0/16:1 and PC O-18:1/16:1) and PE P-38:3 (PE P-18:0/20:3 and PE

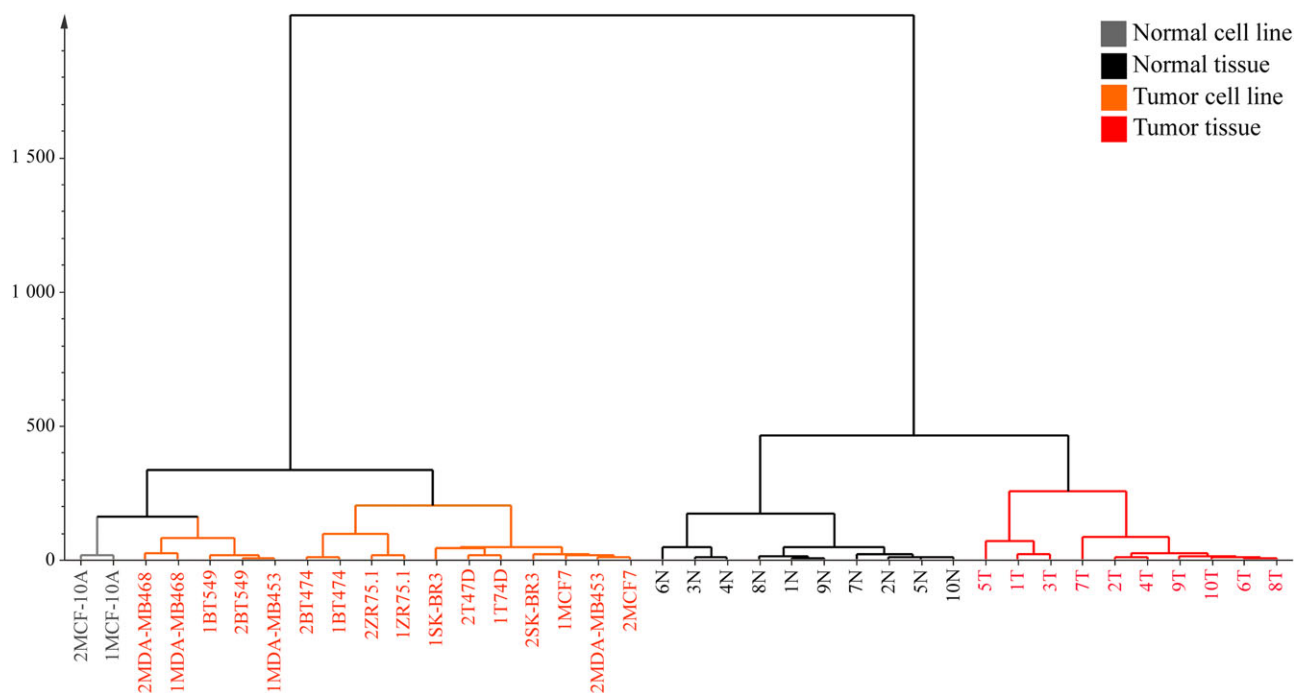


Figure 6. Dendrogram of normal and tumor breast cell lines and tissues calculated using the Ward linkage criterion.

O-18:1/20:3). The most abundant fatty acyl combinations on the glycerol skeleton were identified by MS/MS spectra in the negative-ion ESI mode.

### Correlation of breast cell lines and breast tissues of cancer patients

LC/MS analysis enables the identification and characterization of differences in the lipidomic composition (see Supplementary Table S2, Supporting Information) of the breast normal cell line (MCF10A) and nine breast tumor cell lines (ZR-75-1, T-74D, MCF7, MDA-MB-231, MDA-MB-453, MDA-MB-468, SK-BR-3, BT-474 and BT-549). In our previous work we described changes in the lipidome of breast tumor tissue and surrounding normal tissue of breast cancer patients using the same LC/MS method.<sup>[24]</sup> However, these changes in breast tissues could also be caused by other factors in addition to cancer, such as inflammation and immune response. Moreover, the information is also diluted due to the presence of other cell types, adipose tissue, ducts, etc. On the other hand, the comparison of cell lines (tumor *vs.* normal) provides undiluted information on the lipidomic changes occurring in

the tumor cell after the transformation from the normal cell. The goal of the present work is to determine the degree of similarity between tumor cell lines and tumor tissues and mainly to identify the most dysregulated lipids observed for both models.

Various MDA approaches are used for the statistical evaluation of relative abundances of 123 lipids from four lipid classes determined in this work: PCA, HCA, OPLS-DA, S-plots, dendrogram and ROC curves. The gap between cell lines (on the left) and tissues (on the right) in the PCA plot shown in Fig. 5(A) confirms the initial expectation that differences between cell lines and tissues are not negligible, but it is still possible to distinguish cancer samples from normal samples even in this unsupervised PCA plot. The same conclusion is obtained from the HCA plot as the second unsupervised MDA method that the primary separation criterion is the type of sample (cell line *vs.* tissue) and the second is cancer *vs.* normal (Fig. 6). When we switch from unsupervised methods to supervised OPLS-DA, then of course the group resolution is significantly improved and cancer *vs.* normal samples are clearly distinguished in all cases (Fig. 5(B)). The next step is the identification of most

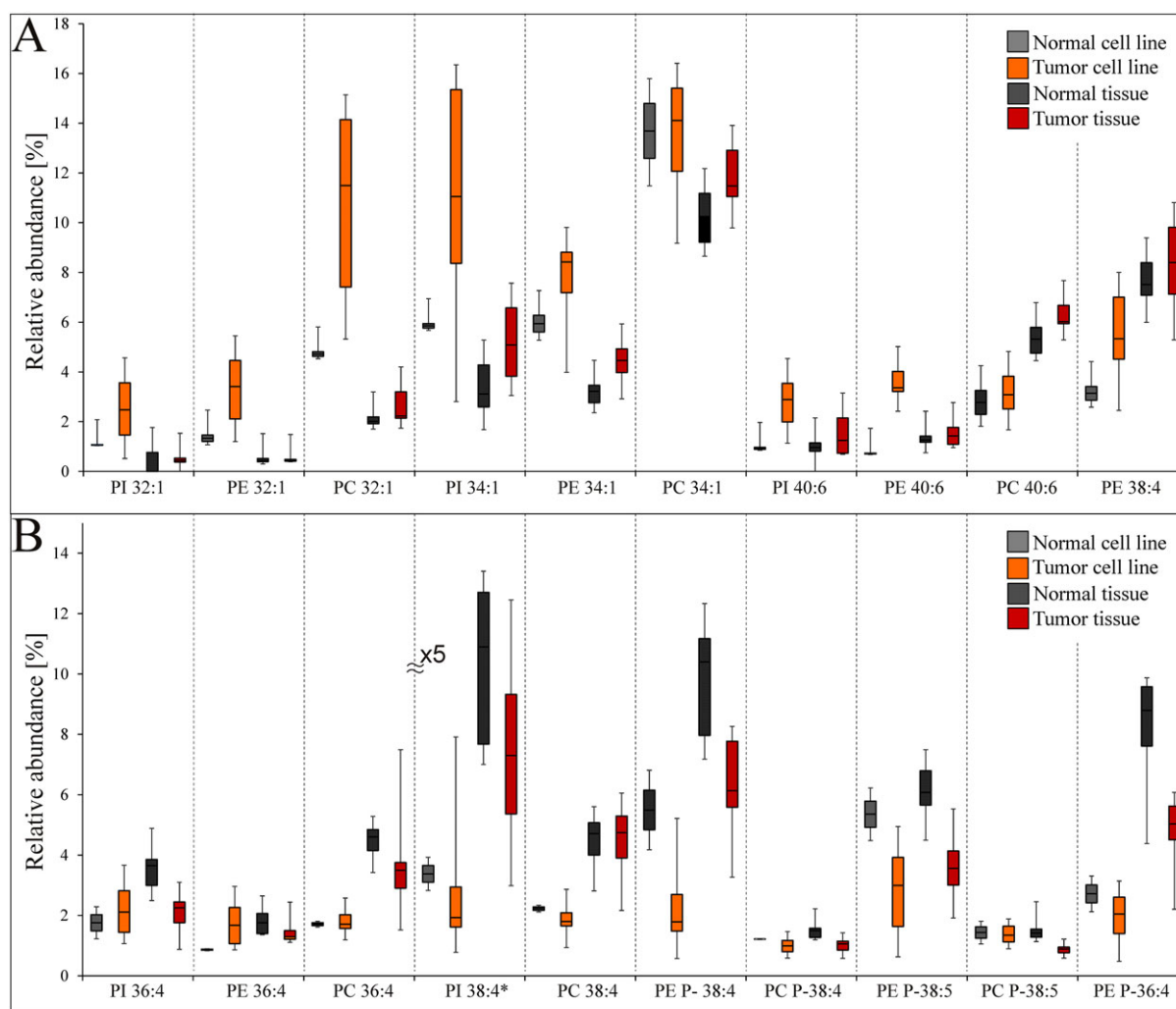


**Figure 7.** Box plots describing the most important (A) upregulated and (B) downregulated lipids in normal and tumor breast cell lines and tissues of breast cancer patients. \*In the case of PI 38:4,  $y$  axes values are five times more than shown numbers, i.e., 0–70% range.

dysregulated lipids valid for both models using an S-plot (Fig. 5(C)). The logical series of the 10 most upregulated (Fig. 7(A)) and 10 most downregulated (Fig. 7(B)) lipids are visualized by box plots with intervals of their relative abundances for all sample types. The central line in the box plot (Fig. 7) shows the value of the median, the lower part represents the first quartile and the upper part the third quartile. Extreme lines show minimum and maximum values. Some trends can be generalized and they are also in agreement with the state-of-the-art knowledge of lipidomic changes related to cancer. The significant upregulation is evident (Fig. 5(C)) for lipids containing saturated and monounsaturated fatty acyls with shorter chains (32:0, 32:1, 34:0 and 34:1), which is illustrated in Fig. 7(A) for logical series of PL 32:1 and 34:1, but less pronounced upregulation could be observed for other low unsaturated PL as well. This is in perfect agreement with GC/MS data shown in Fig. 3 and Supplementary Fig. S5 (Supporting Information). Some PL with highly PUFA are upregulated (PI 40:6, PE 40:6, PC 40:6 and PE 38:4), while other polyunsaturated PL with general formulas 36:4 and 38:4 (combinations of 16:0/20:4 and 18:0/20:4) are downregulated (see Fig. 7(B)). The exception is the behavior of PE 38:4. It is clear that PL containing PUFA have important roles in cancer and changes could be also expected in the area of oxylipins formed by the oxidation of PUFA chains released from corresponding PL. Another general effect is the significant downregulation of ether and plasmalogen PE and PC, as shown in some examples in Fig. 7(B) and for the sum of all PE ethers and plasmalogens in Supplementary Fig. S6 (Supporting Information). Another way of visualization of the potential of most dysregulated lipids for distinguishing cancer *vs.* normal groups is the use of ROC curves (Supplementary Fig. S7, Supporting Information), which provides information on false positive/false negative rates. The area under the curve (AUC) in ROC graphs is a measure of reliability of used parameter for the differentiation of tumor *vs.* normal states. We plot sums of PE 32:1 + PI 32:1 + PC 32:1 in Supplementary Figs. S7(A) and S7(B) (Supporting Information) and of PE 36:4 + PI 36:4 + PC 36:4 in Supplementary Figs. S7(C) and S7(D) for cell lines (Figs. 7(A) and 7(C)) and tissues (Figs. 7(B) and 7(D)). The absolute resolution is obtained for PL 32:1 in cell lines (AUC = 1.00), but significantly decreased for tissues (AUC = 0.70), while results for PL 36:4 are comparable in both cases (AUC = 0.81 and 0.90, respectively).

## CONCLUSIONS

This work confirms that changes observed in breast tumor tissues are caused mainly by different lipidomic profiles of tumor cells and these changes can be well correlated with the lipidomic composition of the nine breast cancer cell lines studied here. Although individual breast cancer cell lines show some differences in their lipidomic profiles, these differences do not cause problems in the differentiation between tumor and normal cells. The current research will continue with the analysis of human plasma of cancer patients and healthy volunteers with the emphasis on dysregulated lipids identified in tumor cell lines and tumor tissues and comparison between different types of breast cancer. Differences in lipid concentrations between normal and cancer

groups are rather small for human plasma; therefore, the information on cancer-induced dysregulation of some PL with low unsaturation level (mainly 32:1 and 34:1), PL containing PUFA (36:4, 38:4, 38:5, 40:6, etc.) and plasmalogen and other ether lipids observed in cell lines and tissues could be helpful for the targeted lipidomic profiling of human plasma. These changes are also in agreement with GC/MS data showing the upregulation of shorter saturated (14:0 and 16:0) and monounsaturated (16:1) fatty acyls and some PUFA (20:4, 22:5 and 22:6).

## Acknowledgements

This work was supported by the ERC CZ grant project LL1302 sponsored by the Ministry of Education, Youth and Sports of the Czech Republic. R.H. acknowledges the support of MEYS – NPS I – LO1413 and MH CZ - DRO (MMCI, 00209805) projects. The help of Blanka Červená and Magdaléna Ovčáčiková (University of Pardubice) with the sample extraction is acknowledged.

## REFERENCES

- [1] D. Barh, A. Carpi, M. Verma, M. Gunduz. *Cancer Biomarkers: Minimal and Noninvasive Early Diagnosis and Prognosis*. CRC Press, Boca Raton, FL, USA, 2014.
- [2] *The Molecular Biology of Cancer*, (Eds: S. Pelengaris, M. Khan), (2nd edn.). Wiley-Blackwell, Oxford, UK, 2013.
- [3] B. Melichar, H. Studentova, H. Kalabova, D. Vitaskova, P. Cermakova, H. Hornychova, A. Ryska. Predictive and prognostic significance of tumor-infiltrating lymphocytes in patients with breast cancer treated with neoadjuvant systemic therapy. *Anticancer Res.* 2014, 34, 1115.
- [4] B. Melichar. Laboratory medicine and medical oncology: the tale of two Cinderellas. *Clin. Chem. Lab. Med.* 2013, 51, 99.
- [5] J. Baumann, C. Sevensky, D. S. Conklin. Lipid biology of breast cancer. *Biochim. Biophys. Acta Mol. Cell Biol. Lipids* 2013, 1831, 1509.
- [6] S. F. Nabavi, S. Bilotto, G. L. Russo, I. E. Orhan, S. Habtemariam, M. Daglia, K. P. Devi, M. R. Loizzo, R. Tundis, S. M. Nabavi. Omega-3 polyunsaturated fatty acids and cancer: lessons learned from clinical trials. *Cancer Metastasis Rev.* 2015, 34, 359.
- [7] E. Rysman, K. Brusselmans, K. Scheys, L. Timmermans, R. Derua, S. Munck, P. P. Van Veldhoven, D. Waltregny, V. W. Daniels, J. Machiels, F. Vanderhoydonc, K. Smans, E. Waelkens, G. Verhoeven, J. V. Swinnen. De novo lipogenesis protects cancer cells from free radicals and chemotherapeutics by promoting membrane lipid saturation. *Cancer Res.* 2010, 70, 8117.
- [8] C. R. Santos, A. Schulze. Lipid metabolism in cancer. *FEBS J.* 2012, 279, 2610.
- [9] M. P. Wymann, R. Schneider. Lipid signalling in disease. *Nat. Rev. Mol. Cell Biol.* 2008, 9, 162.
- [10] S. M. Louie, L. S. Roberts, M. M. Mulvihill, K. X. Luo, D. K. Nomura. Cancer cells incorporate and remodel exogenous palmitate into structural and oncogenic signaling lipids. *Biochim. Biophys. Acta Mol. Cell Biol. Lipids* 2013, 1831, 1566.
- [11] M. Hilvo, C. Denkert, L. Lehtinen, B. Muller, S. Brockmoller, T. Seppanen-Laakso, J. Budczies, E. Bucher, L. Yetukuri, S. Castillo, E. Berg, H. Nygren, M. Sysi-Aho, J. L. Griffin, O. Fiehn, S. Loibl, C. Richter-Ehrenstein, C. Radke, T. Hyotylainen, O. Kallioniemi, K. Iljin, M. Oresic. Novel

- theranostic opportunities offered by characterization of altered membrane lipid metabolism in breast cancer progression. *Cancer Res.* **2011**, *71*, 3236.
- [12] W. W. Lv, T. S. Yang. Identification of possible biomarkers for breast cancer from free fatty acid profiles determined by GC-MS and multivariate statistical analysis. *Clin. Biochem.* **2012**, *45*, 127.
- [13] N. Azordegan, V. Fraser, K. Le, L. M. Hillyer, D. W. L. Ma, G. Fischer, M. H. Moghadasian. Carcinogenesis alters fatty acid profile in breast tissue. *Mol. Cell. Biochem.* **2013**, *374*, 223.
- [14] P. A. Corsetto, G. Montorfano, S. Zava, I. E. Jovenitti, A. Cremona, B. Berra, A. M. Rizzo. Effects of n-3 PUFAs on breast cancer cells through their incorporation in plasma membrane. *Lipids Health Dis.* **2011**, *10*.
- [15] M. C. Pender-Cudlip, K. J. Krag, D. Martini, J. Yu, A. Guidi, S. S. Skinner, Y. Zhang, X. Y. Qu, C. W. He, Y. Xu, S. Y. Qian, J. X. Kang. Delta-6-desaturase activity and arachidonic acid synthesis are increased in human breast cancer tissue. *Cancer Sci.* **2013**, *104*, 760.
- [16] C. G. Skibinski, A. Das, K. M. Chen, J. Liao, A. Manni, M. Kester, K. El-Bayoumy. A novel biologically active acid stable liposomal formulation of docosahexaenoic acid in human breast cancer cell lines. *Chem.-Biol. Interact.* **2016**, *252*, 1.
- [17] T. R. Witte, W. E. Hardman. The effects of omega-3 polyunsaturated fatty acid consumption on mammary carcinogenesis. *Lipids* **2015**, *50*, 437.
- [18] J. X. Kang, A. Liu. The role of the tissue omega-6/omega-3 fatty acid ratio in regulating tumor angiogenesis. *Cancer Met. Rev.* **2013**, *32*, 201.
- [19] J. Bergan, T. Skotland, T. Sylvanne, H. Simolin, K. Ekroos, K. Sandvig. The ether lipid precursor hexadecylglycerol causes major changes in the lipidome of HEp-2 cells. *PLoS One* **2013**, *8*.
- [20] M. L. Doria, C. Z. Cotrim, C. Simoes, B. Macedo, P. Domingues, M. R. Domingues, L. A. Helguero. Lipidomic analysis of phospholipids from human mammary epithelial and breast cancer cell lines. *J. Cell. Physiol.* **2013**, *228*, 457.
- [21] M. L. Doria, Z. Cotrim, B. Macedo, C. Simoes, P. Domingues, L. Helguero, M. R. Domingues. Lipidomic approach to identify patterns in phospholipid profiles and define class differences in mammary epithelial and breast cancer cells. *Breast Cancer Res. Tr.* **2012**, *133*, 635.
- [22] H. Kim, H. K. Min, G. Kong, M. H. Moon. Quantitative analysis of phosphatidylcholines and phosphatidylethanolamines in urine of patients with breast cancer by nanoflow liquid chromatography/tandem mass spectrometry. *Anal. Bioanal. Chem.* **2009**, *393*, 1649.
- [23] L. Yang, X. G. Cui, N. N. Zhang, M. Li, Y. Bai, X. H. Han, Y. K. Shi, H. W. Liu. Comprehensive lipid profiling of plasma in patients with benign breast tumor and breast cancer reveals novel biomarkers. *Anal. Bioanal. Chem.* **2015**, *407*, 5065.
- [24] E. Cífková, M. Holčápek, M. Lísa, D. Vrána, J. Gatěk, B. Melichar. Determination of lipidomic differences between human breast cancer and surrounding normal tissues using HILIC-HPLC/ESI-MS and multivariate data analysis. *Anal. Bioanal. Chem.* **2015**, *407*, 991.
- [25] L. Eriksson, T. Byrne, E. Johansson, J. Trygg, C. Vikström. *Multi- and Megavariate Data Analysis. Basic Principles and Applications*, (3rd revised edn.). MKS Umetrics AB, Malmö, Sweden, **2013**.
- [26] G. Liebisch, J. A. Vizcaino, H. Kofeler, M. Trotschmuller, W. J. Griffiths, G. Schmitz, F. Spener, M. J. O. Wakelam. Shorthand notation for lipid structures derived from mass spectrometry. *J. Lipid Res.* **2013**, *54*, 1523.
- [27] J. Folch, M. Lees, G. H. S. Stanley. A simple method for the isolation and purification of total lipids from animal tissues. *J. Biol. Chem.* **1957**, *226*, 497.
- [28] M. Lísa, E. Cífková, M. Holčápek. Lipidomic profiling of biological tissues using off-line two-dimensional high-performance liquid chromatography mass spectrometry. *J. Chromatogr. A* **2011**, *1218*, 5146.
- [29] S. Hamilton, R. J. Hamilton, P. A. Sewell. *Lipid Analysis: Practical Approach*, Oxford University Press, NY, **1992**.
- [30] E. Cífková, M. Holčápek, M. Lísa, M. Ovčáčiková, A. Lyčka, F. Lynen, P. Sandra. Nontargeted quantitation of lipid classes using hydrophilic interaction liquid chromatography-electrospray ionization mass spectrometry with single internal standard and response factor approach. *Anal. Chem.* **2012**, *84*, 10064.

## SUPPORTING INFORMATION

Additional supporting information may be found in the online version of this article at the publisher's website.